THE JOURNAL OF PHYSICAL CHEMISTRY B

ARTICLE

pubs.acs.org/JPCB

Stereoselectivity for DNA Threading Intercalation of Short Binuclear Ruthenium Complexes

Johanna Andersson and Per Lincoln*

Department of Chemical and Biological Engineering, Chalmers University of Technology, SE-41296 Gothenburg, Sweden

Supporting Information

ABSTRACT: Threading intercalation is an unusual DNA binding mode with significantly slower association and dissociation rates compared with classical intercalation. The latter has been shown to correlate well with cytotoxicity, and therefore, threading intercalating compounds are of great interest in the search for new DNA binding drugs. Thus, there is a need for better understanding of the mechanisms behind this type of binding. In this work, we have investigated the threading intercalation ability of the four stereoisomers of the AT-specific binuclear ruthenium complex $[\mu\text{-dppzip(phen)}_4\text{Ru}_2]^{4+}$ using different spectroscopic techniques. This complex contains an unsymmetrical bridging ligand consisting of a dipyridophenazine and an imidazophenanthroline ring system, in which the photophysical properties of the Ru-dipyridophenazine complex moiety make it possible to distinguish the intercalating part from the nonintercalating part. We have found that Δ geometry around the ruthenium on the intercalating dipyridophenazine moiety and Λ geometry on the nonintercalating imidazophenanthroline moiety is the optimal configuration for threading intercalation of this complex and that the chirality on the ruthenium of the nonintercalating half dominates the stereospecificity in the threaded state. This is the cause of the reversed enantioselectivity compared with the parent threading intercalating complex $[\mu\text{-bidppz-(phen)}_4\text{Ru}_2]^{4+}$, in which the enantioselectivity is controlled by the chirality on the intercalating half. The differences in the interactions with DNA between the two complexes are most likely due to the fact that $[\mu\text{-dppzip(phen)}_4\text{Ru}_2]^{4+}$ has a slightly shorter bridging ligand than the parent complex.

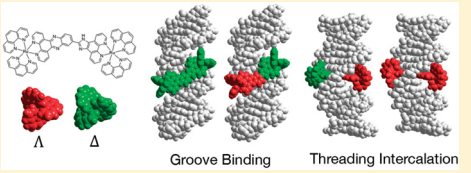

INTRODUCTION

Threading intercalation is an unusual DNA binding mode observed for molecules containing an aromatic ring system with bulky substituents on opposite ends, for example, nogalamycin.[1−4] In the bound state, the flat middle part is intercalated between the base pairs, and the bulky substituents are located one in each groove. For binding as well as dissociation from the bound state to occur, one of the bulky substituents has to be passed through the base pair stack, a process that requires severe distortions of the DNA structure and, in some cases, probably even transient opening of at least one base pair.[2] As a result, threading intercalating compounds display reduced association and dissociation rates compared with their nonthreading analogues. The latter, in particular, has been shown to be important for cytotoxic activity, making threading intercalating compounds interesting in the search for new DNA binding drugs.[1,5] Moreover, threading intercalation usually displays large differences in association and dissociation rates between AT and GC base pairs in double-stranded DNA[1,2,6,7] and preferentially occurs at bulged sites in RNA structures,[8,9] providing some degree of inherent sequence selectivity. Because sequence specificity is crucial for DNA binding drugs to target diseases other than cancer and to minimize side effects, this further increases the interest for threading intercalating compounds, and efforts have been made to target more specific sequences by designing the bulky side groups in such a way that they interact with unique base pair patterns in the grooves.[10−14]

Threading intercalating ruthenium complexes have been shown to have significantly slower kinetics than other synthetic threading intercalators. $[\mu\text{-bidppz(phen)}_4\text{Ru}_2]^{4+}$ (phen = 1,10-phenanthroline, bidppz = 11,11′-bi(dipyrido[3,2-*a*:2′,3′-*c*]-phenazinyl)) (Chart 1), which was one of the first discovered threading intercalating ruthenium complexes, displays outstandingly slow dissociation with rate constants of $10^{-3}-10^{-4}$ s^{-1} which is in the same range as for the natural cytotoxic threading intercalator nogalamycin.[1,15] Interestingly, $[\mu\text{-bidppz(phen)}_4\text{Ru}_2]^{4+}$ also binds selectively to long AT sequences (≥14 consecutive base pairs) due to kinetic control of the threading interaction.[6,16] Because of its extremely slow dissociation and AT selectivity, $[\mu\text{-bidppz(phen)}_4\text{Ru}_2]^{4+}$ has been studied as a model compound for threading intercalation, aiming for a deeper understanding of the threading mechanism.[6,16−19]

Recently, we have synthesized a number of related ruthenium complexes to investigate how complex structure affects threading intercalation ability, which resulted in the discovery of a new threading intercalating compound, $[\mu\text{-dppzip(phen)}_4\text{Ru}_2]^{4+}$ (dppzip = 2-(dipyrido[3,2-*a*:2′,3′-*c*]phenazin-11-yl)-imidazo-[4,5-*f*]-1,10-phenanthroline) shown in Chart 1.[20] $[\mu\text{-dppzip-(phen)}_4\text{Ru}_2]^{4+}$ has an unsymmetrical bridging ligand consisting of one dipyridophenazine (dppz) moiety and one imidazophenanthroline (ip) moiety connected by a single bond, resulting in a slightly shorter distance between the two ruthenium ions compared with $[\mu\text{-bidppz(phen)}_4\text{Ru}_2]^{4+}$ (18 versus 19 Å, as

Received: July 3, 2011
Revised: October 17, 2011
Published: October 19, 2011

Chart 1. Structures of DNA Threading Intercalating Ruthenium Complexes

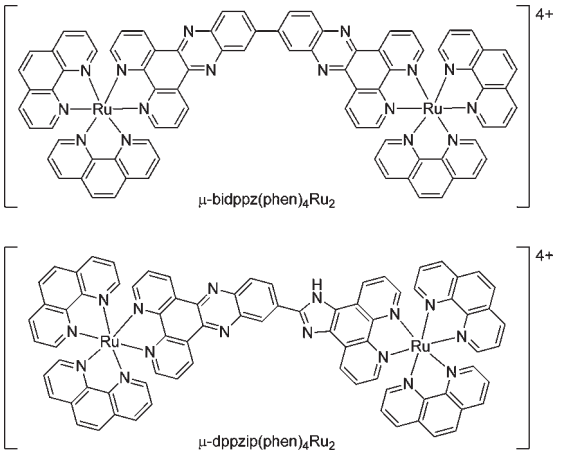

determined from PM3-optimized structures). In contrast to $[\mu\text{-bidppz(phen)}_4\text{Ru}_2]^{4+}$, which although being kinetically selective for AT-DNA still binds mixed sequence DNA to some extent, $[\mu\text{-dppzip(phen)}_4\text{Ru}_2]^{4+}$ intercalates only AT-DNA. Interestingly, we also found that the ΛΛ enantiomer of $[\mu\text{-dppzip(phen)}_4\text{Ru}_2]^{4+}$ (**ΛΛ**) is a more efficient threading intercalator than the ΔΔ enantiomer (**ΔΔ**), which is opposite to what has been observed for the parent compound in which the ΔΔ enantiomer is more efficient. To investigate the mechanism behind this reversed enantioselectivity and how the chirality around the ruthenium center affects threading intercalation ability, we have in this work synthesized and studied the DNA binding properties also of the "meso" enantiomeric pair of $[\mu\text{-dppzip(phen)}_4\text{Ru}_2]^{4+}$, which we here denote **ΔΛ** and **ΛΔ**, where the first and second symbols describes the chirality on the dppz and ip part of the complex, respectively.

EXPERIMENTAL METHODS

Sample preparation. The ΔΛ and ΛΔ isomers of $[\mu\text{-dppzip(phen)}_4\text{Ru}_2]^{4+}$ were synthesized from homochiral Ru(phen)$_2$(1,10-phenanthrolin-5,6-dione) hexafluorophosphate according to the same procedure as previously reported for the ΔΔ and ΛΛ isomers.[20]

All experiments were performed in 1 mM sodium cacodylate buffer, pH 7.0, containing 150 mM NaCl. Stock solutions of the complexes were prepared by dissolving the chloride salts in Milli-Q water. Stock solutions (~5 mM) of $[\text{poly(dAdT)}]_2$ were prepared by dissolving the sodium salt purchased from Amersham Biosciences (LD) and Sigma-Aldrich (all other experiments) in buffer. A stock solution (~5 mM) of ct-DNA was prepared by dissolving highly polymerized type I sodium salt calf thymus DNA (Sigma-Aldrich) in buffer. The solution was filtered two times through a 0.7 μm polycarbonate filter. Steady state spectra and association kinetics were measured at a concentration of 3.75 μM complex and 120 μM DNA obtained by 1:1 mixing of complex and DNA solutions of appropriate concentrations. Dissociation kinetics was studied by addition of a 3% (w/w) solution of sodium dodecyl sulfate (SDS) in buffer to equilibrated samples of complex (3.75 μM) and DNA (120 μM) to a final concentration of 0.6% SDS. Concentrations were determined spectrophotometrically using ε_{263} = 200 000 M^{-1} cm^{-1} for $[\mu\text{-dppzip(phen)}_4\text{Ru}_2]^{4+}$, ε_{262} = 6600 M^{-1} cm^{-1} for $[\text{poly(dAdT)}]_2$ and ε_{258} = 6600 M^{-1} cm^{-1} for calf thymus DNA. The DNA concentrations are given in nucleotides.

Instrumentation. Absorption spectra were recorded on a Varian Cary 4000 or a Varian Cary 5000 UV/vis spectrophotometer with buffer as baseline. Circular dichroism (CD) spectra were recorded on a Chirascan CD spectropolarimeter with buffer as baseline. In general, five CD spectra were averaged for each sample. Linear dichroism (LD) was measured on a Chirascan LD spectropolarimeter on samples oriented in an outer-rotating Couette flow cell with a 1 mm path length at a shear flow gradient of 3000 s^{-1}. Spectra were corrected for baseline contributions by subtraction of the corresponding spectra recorded without rotation.

Binding and dissociation kinetics were studied using a Varian Cary Eclipse spectrofluorometer equipped with a multicell temperature controller. The samples were excited at 460 nm, and the change in emission intensity was studied at 625 nm. Binding kinetics was also investigated by studying the change in CD signal at 485 nm using a Chirascan CD spectropolarimeter.

Nanosecond emission decays were measured by using the third harmonic of a Nd:YAG laser (Continuum Surelite II-10, pulse width <7 ns) to provide an excitation wavelength of 355 nm. The emitted light was detected with a Hamamatsu R928 photomultiplier tube at an angle of 90° relative to the excitation light. The monitoring wavelength was set to 630 nm. The decays were collected and averaged with a 200 MHz digital oscilloscope (Tetronix TDS2200 2Gs/s) and stored in a Lab View program (developed at the department), which also controls the instrument setup. Forty-eight decay curves were averaged for each sample. Steady state emission spectra were recorded on a Varian Cary Eclipse at an excitation wavelength of 460 nm and normalized against the corresponding emission spectra recorded at 355 nm excitation, where all samples had equal absorbance.

Data Analysis. The association and dissociation kinetic traces were projected onto the space spanned by one, two or three exponentials using the matrix pseudoinverse function *pinv* in the Matlab software package (Mathworks, Inc.; www.mathworks.com). The (Euclidian) norm of the residual was minimized by varying the rate constants with the simplex algorithm using the Matlab function *fminsearch*. A fit was judged acceptable if the residual was unstructured and inclusion of an additional exponential did not decrease the residual norm by more than 30%. Dissociation kinetic traces were corrected for dilution effects before analysis.

The emission decays were analyzed as described above for the kinetic traces, and all traces were found to be biexponential. Due to their similarity, the rate constants of two exponentials were simultaneously optimized to the decays for **ΔΛ** and **ΛΔ** as well as to the decays of **ΔΔ** and **ΛΛ**. The relative quantum yields were obtained by integration of the emission spectra on the energy scale using the *trapz* function in Matlab.

Linear dichroism[21] is defined as the difference in absorbance of linearly polarized light, parallel and perpendicular to a macroscopic orientation axis (here the DNA helix axis):

$$\text{LD} = A_{\parallel} - A_{\perp} \quad (1)$$

The reduced linear dichroism (LD^r) is the LD divided by the isotropic absorption. From the LD^r, the angle α between the orientation axis and the transition dipole moment of an oriented chromphore can be calculated from eq 2 for nonoverlapping absorption bands, provided that the global orientation factor $0 \le S \le 1$, which here measures how well the DNA helix axis

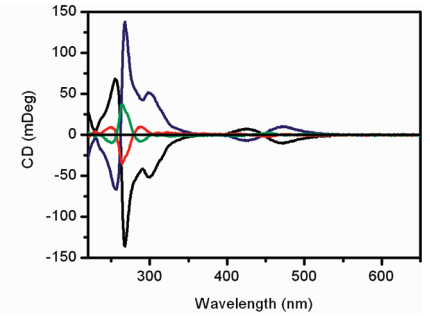

Figure 1. CD spectra of **ΔΔ** (black), **ΔΛ** (red), **ΛΔ** (green), and **ΛΛ** (blue) in buffer. The concentration of the complex was 3.75 μM.

is aligned in the shear flow created in the Couette flow cell, can be determined. An estimate for S can be obtained from the LD^r in the nucleobase absorption region around 260 nm, assuming $\alpha = 90°$ for the $\pi \rightarrow \pi^*$ transitions.

$$LD^r = LD/A_{iso} = 1.5S(3\cos^2\alpha - 1) \quad (2)$$

RESULTS

Characterization of the New Stereoisomers. The absorption spectra of the new "meso"-enantiomeric pair of $[\mu$-dppzip$(phen)_4Ru_2]^{4+}$ in buffer solution are identical to those of the homochiral pair **ΔΔ** and **ΛΛ** (see Figure S1 of the Supporting Information). The circular dichroism (CD) spectra of **ΔΛ** and **ΛΔ** when free in buffer solution are shown in Figure 1. Despite the fact that those isomers contain one Δ and one Λ ruthenium center, whose CD theoretically would cancel out for a symmetrical complex, their CD is nonzero below 550 nm, which is probably due to differences in the coupling between the phenanthroline ligands on the two ruthenium centers and the dppz and ip part of the bridging ligand, respectively. Comparison of the CD spectra of the homochiral stereoisomers of $[\mu$-dppzip$(phen)_4Ru_2]^{4+}$ and $[\mu$-bidppz$(phen)_4Ru_2]^{4+}$ indicates that the dppz side shows a sharper CD band than that of the ip side, which appears broadened, perhaps due to a relatively free rotation around the dppz-ip pivot bond.

Binding Geometry. The absorption spectra of all four stereoisomers display a hypochromic shift in the visible region upon addition of AT-DNA to the complexes, as previously reported for **ΔΔ** and **ΛΛ**.[20] Upon incubation at 50 °C, the absorbance in the visible region decreases even further, with **ΔΛ** displaying the largest changes. Interestingly, the spectra of **ΔΛ** and **ΛΛ** also become more structured, as shown in Figure 2, whereas the shape of the spectra in the visible region remain virtually the same for **ΛΔ** and **ΔΔ**, the stereoisomers with Δ-configuration at the ip part.

Linear dichroism measures the difference in absorbance of linearly polarized light parallel and perpendicular to a macroscopic orientation axis (here, the DNA helix axis) and is a sensitive tool to probe differences in binding geometry of small DNA bound chromophores. From the LD^r, which is the LD divided by the isotropic absorbance, the angle between the transition dipole moment and the DNA helix axis can be calculated, provided that the orientation factor is known for the sample. A negative LD^r value corresponds to a more perpendicular orientation of the transition dipole moment relative the DNA helix axis, and a positive LD^r value corresponds to a more parallel orientation. As seen in Figure 3a, the LD^r spectra immediately after mixing with AT-DNA are virtually identical for all four isomers, indicating

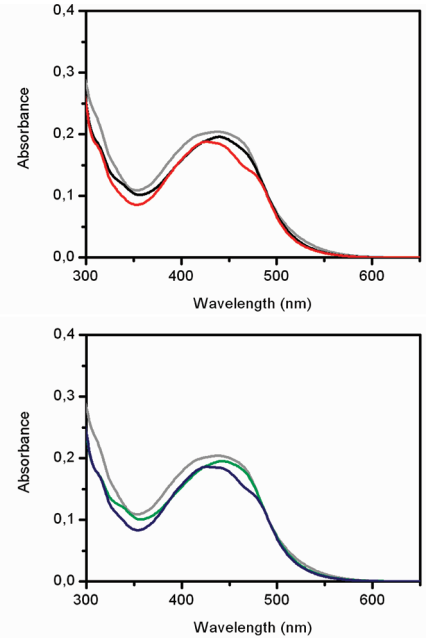

Figure 2. Absorption spectra of **ΔΔ** (black), **ΔΛ** (red), **ΛΔ** (green), and **ΛΛ** (blue) in the presence of AT-DNA at equilibrium. The spectra of the complex free in buffer solution are shown in gray.

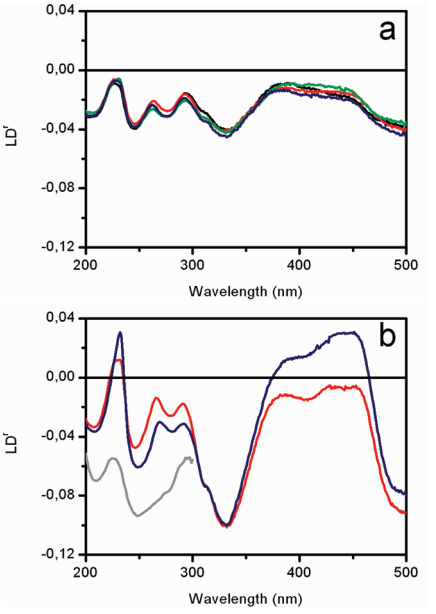

Figure 3. (a) LD^r spectra of **ΔΔ** (black), **ΔΛ** (red), **ΛΔ** (green), and **ΛΛ** (blue) in the presence of AT-DNA immediately after mixing. (b) LD^r spectra of at **ΔΛ** (red), **ΛΛ** (blue) at equilibrium. The LD^r of free DNA is shown in gray. The concentrations of complex and DNA were 3.75 and 120 μM, respectively. The LD data has been rescaled to 1 cm path length before division with the absorbance.

similar binding modes for all of them (see Figure S2 of the Supporting Information for LD spectra). The initial LD^r spectra in the presence AT-DNA is also very similar to the LD^r spectra in the presence of ct-DNA (Figure S3 of the Supporting Information). However, although the shape of the LD^r spectra in the presence of ct-DNA remains unchanged with time for all four

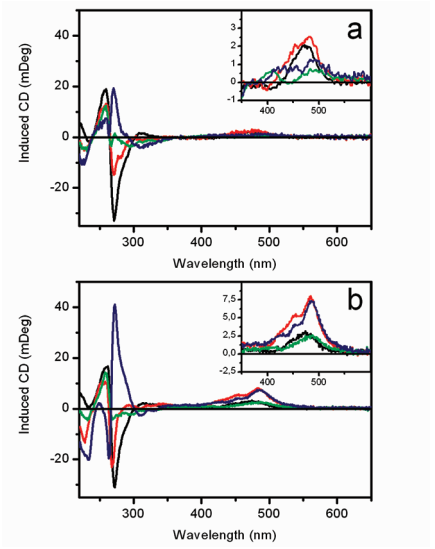

Figure 4. Induced CD for **ΔΔ** (black), **ΔΛ** (red), **ΛΔ** (green), and **ΛΛ** (blue) in the presence of AT-DNA immediately after mixing (a) and at equilibrium (b). The concentration of complex and DNA were 3.75 and 120 μM, respectively.

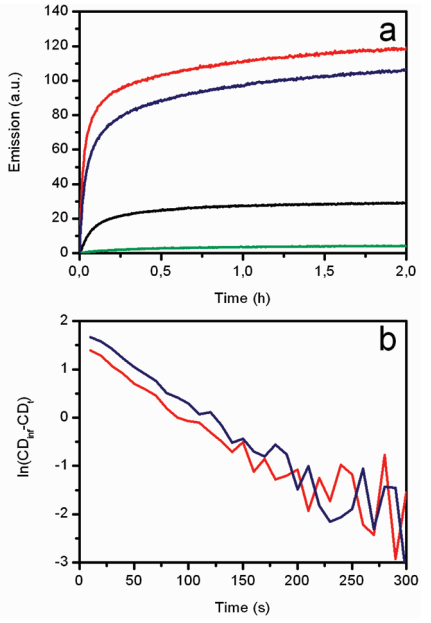

Figure 5. Kinetic traces for association at 50 °C of **ΔΔ** (black), **ΔΛ** (red), **ΛΔ** (green), and **ΛΛ** (blue) in the presence of AT-DNA studied by (a) fluorescence spectroscopy and (b) CD. The concentrations of the complex, DNA, and NaCl were 3.75 μM; 120 μM; and 150 mM, respectively. The emission intensity at the first data point after addition of DNA to the samples has been subtracted from all data points to facilitate comparison of the change in emission intensity.

isomers, the shape of the spectra in the presence of AT-DNA changes dramatically for **ΔΛ** and **ΛΔ** upon incubation at 37 °C (Figure 3b). The bridging ligand $\pi \rightarrow \pi^*$ and MLCT band at 325 and 485 nm, respectively, become more negative after incubation, indicating rearrangement from a binding mode with a smaller angle between the DNA helix axis and the long axis of the bridging ligand to a more perpendicular orientation of the bridging ligand. For **ΔΔ** and **ΛΛ**, on the other hand, the shape of the LD and LD^r remains essentially the same after incubation at 37 °C, although the orientation of the DNA decreases substantially (Figure S4 of the Supporting Information). This is probably not only an effect of the 37 °C incubation, as this treatment sometimes increases the orientation of pure DNA, but may be an effect of the Δ-ip moiety, which as part of a binuclear bisimidazophenanthroline benzene complex has been shown to effectively compact DNA.[20]

The changes in binding mode were studied also with circular dichroism, in which the results are not affected by differences in orientation of the sample. Immediately after mixing with both ct- and AT-DNA, all four stereoisomers exhibit a weak, positive, induced CD in the visible region (Figure 4a and Figure S5 of the Supporting Information). There is a small but significant difference in induced CD in the visible region between the isomers with the Δ configuration on the dppz part and the ones with the Λ configuration, but considering the fact that the dppz part seems to dominate the CD for the whole complex, this supports similar binding modes for all four stereoisomers. Upon incubation at 37 °C in the presence of AT-DNA, a small but significant increase in induced CD at 485 nm is observed for **ΔΔ** and **ΛΛ**, whereas more dramatic changes are observed for **ΔΛ** and **ΛΔ** (Figure 4b). A strong, positive, induced CD in the visible region has previously been shown to be associated with threading intercalation of the parent $[\mu$-bidppz(phen)$_4$Ru$_2]^{4+}$ complex[18] and suggests that threading intercalation of all four isomers indeed occurs with AT-DNA. However, only a fraction of **ΔΔ** and **ΛΛ** seem to bind by threading intercalation because the changes in induced CD are much smaller compared with the other two isomers. In the presence of ct-DNA, the CD spectra remained unchanged for all isomers after incubation at 37 °C, which confirms the previous conclusion that $[\mu$-dppzip(phen)$_4$Ru$_2]^{4+}$ does not bind ct-DNA by threading intercalation.

Kinetics. As previously reported, $[\mu$-dppzip(phen)$_4$Ru$_2]^{4+}$ is quenched in aqueous solution but becomes brightly luminescent upon binding to DNA by threading intercalation,[20] enabling studies of the threading process by monitoring the luminescence change at 625 nm. Figure 5a shows the kinetic traces obtained at 50 °C, where it is evident that addition of AT-DNA to the complexes results in a slow increase in luminescence that is characteristic for threading intercalation. The amplitude of the luminescence intensity change differs significantly between the complexes, though, indicating differences in the extent of reaction, where binding appears to be most efficient for **ΔΛ**, followed by **ΛΔ**, **ΔΔ**, and finally, **ΛΛ**. Measurements at 25 and 37 °C (Figure S6 of the Supporting Information) yielded similar results, with the kinetics becoming slower with decreasing temperature, though **ΛΛ** does not seem to thread at all at 25 °C.

Three exponentials were required to fit luminescence kinetic data for **ΔΛ** and **ΛΔ**, whereas the data for **ΔΔ** and **ΛΛ** was biexponential, which complicates the comparison of reaction rates of the four complexes. However, it has previously been shown that the threading intercalation of $[\mu$-bidppz(phen)$_4$Ru$_2]^{4+}$ into AT-DNA, which similarly exhibits multiphasic luminescence kinetics, is monoexponential when monitored by CD, which reports only the primary threading step and is less sensitive than luminescence to the subsequent redistribution of threaded complexes on the DNA lattice.[22] Indeed, monoexponential association kinetics was found for **ΔΛ** and **ΛΔ** by following the change in CD signal at 485 nm (Figure 5b). The threading rate constants determined from the CD experiments are presented in Table 1, which shows that the rate is essentially the

dx.doi.org/10.1021/jp2062767 |J. Phys. Chem. B 2011, 115, 14768–14775

Table 1. Association Rate Constants for Threading Intercalation into AT-DNA.[a]

T, °C)	$\Delta\Lambda$, k, 10^{-3} s^{-1}	$\Lambda\Lambda$, k, 10^{-3} s^{-1}
50	19	18
37	10	7.4
25	1.9	1.4

[a] Determined from CD kinetic traces obtained with 3.75 μM complex and 120 μM nucleotides in 150 mM NaCl.

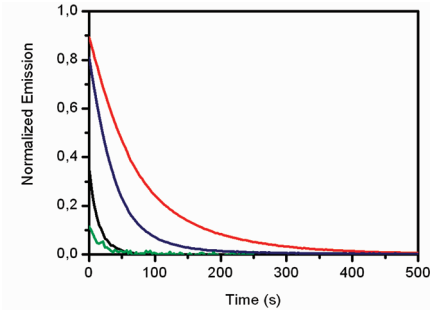

Figure 6. Kinetic traces for dissociation at 50 °C of **ΔΔ** (black), **ΔΛ** (red), **ΛΔ** (green), and **ΛΛ** (blue) from AT-DNA studied by fluorescence spectroscopy. Dissociation was induced by addition of a 3% stock solution of SDS in buffer to equilibrated samples of complex (3.75 μM) and DNA (120 μM) to a final concentration of 0.6% SDS. The kinetic traces have been corrected for dilution effects and are normalized against the luminescence intensity before addition of SDS.

same for **ΔΛ** and **ΛΛ**. The rate constants determined from CD experiments are of the same order of magnitude as those determined for the fastest process in the luminescence experiments, confirming the previous conclusion that the threading event is described by the largest rate constant obtained from luminescence experiments and that the other exponentials arise from redistribution of threaded complexes along the DNA polymer. The change in CD signal at 485 nm was too small for **ΔΔ** and **ΛΔ** to allow kinetic studies, and therefore, no association rate constants are reported for these complexes.

Dissociation kinetics was studied by monitoring the emission decrease at 625 nm after addition of SDS to equilibrated samples of complex and DNA. Measurements were performed at 25, 37, and 50 °C, which all yielded similar results, and the normalized kinetic traces obtained at 50 °C are shown in Figure 6 (see Figure S6 of the Supporting Information for kinetic traces at 25 and 37 °C). As can be seen in Figure 6 there is a significant difference in dissociation between the complexes in which **ΔΛ** has the slowest overall dissociation, followed by **ΛΛ**, **ΔΔ**, and **ΛΔ**. From Figure 6, it is also evident that a large fraction of complex, especially for **ΔΔ** and **ΛΔ**, had dissociated already before data collection had begun. These fast dissociating complexes are probably not bound by threading intercalation but, rather, groove binding/partial intercalation that gives rise to a small increase in luminescence, as has previously been described for other non-intercalating ruthenium complexes.[23]

The kinetic traces for **ΔΛ** and **ΛΛ** were fitted to two exponentials, and the rate constants are presented in Table 2, although the values should be interpreted with caution because SDS has been shown to catalyze the dissociation reaction.[24,25] Both rate constants are rather similar for the two complexes, and it appears that the difference in overall dissociation rate between

Table 2. Dissociation Rate Constants for Threading Intercalation into AT-DNA.[a]

	ΔΛ		ΛΛ	
T, °C	k_1, 10^{-3} s^{-1}(α_1)	k_2, 10^{-3} s^{-1} (α_2)	k_1, 10^{-3} s^{-1}(α_1)	k_2, 10^{-3} s^{-1} (α_2)
50	16 (0.80)	6.5 (0.20)	26 (0.98)	4.6 (0.02)
37	7.6 (0.48)	1.9 (0.52)	8.1 (0.83)	2.2 (0.17)
25	2.8 (0.36)	0.52 (0.64)	3.2 (0.70)	0.76 (0.30)

[a] Determined from luminescence kinetic traces obtained by addition of SDS (3%) to equilibrated samples of 3.75 μM complex and 120 μM nucleotides in 150 mM NaCl to a final concentration of 0.6% SDS.

Table 3. Photophysical Data for the Four Isomers of $[\mu$-dppzip(phen)$_4$Ru$_2]^{4+}$ Bound to AT-DNA

sample[a]	τ_1, ns (α_1)	τ_2, ns (α_2)	τ_{avg}[b], ns	Φ[c]	τ_{rel}[d], ns	% bound[e]
ΔΔ	51 (0.80)	559 (0.20)	153	0.15	1021	17
ΔΛ	54 (0.43)	270 (0.57)	177	1	177	100
ΛΔ	51 (0.77)	559 (0.23)	168	0.11	1550	11
ΛΛ	54 (0.47)	270 (0.53)	168	0.83	202	88

[a] 120 μM nucleotides and 3.75 μM complex in 150 mM NaCl at 25 °C. [b] The average emission lifetime calculated as $\tau_{avg} = \alpha_1\tau_1 + \alpha_2\tau_2$. [c] Relative quantum yields calculated by normalization of the integrated emission spectra against the integrated spectrum for **ΔΛ**. [d] Relative intrinsic lifetimes calculated from $\tau_{rel} = \tau_{avg}/\Phi$. [e] The percentage of bound complex is based on the assumptions that all **ΔΛ** is bound and that the intrinsic lifetime is the same for all isomers, and is calculated as the ratio between τ_{rel} for **ΔΛ** and τ_{rel} for the complex.

these complexes is an effect of different proportions of the fast and slow processes rather than a difference in rate constants. We ascribe both rate constants to threaded complexes because both processes are much slower than what is observed for dissociation of groove bound complex, and we propose that they arise from complexes bound isolated and in close contact with other complexes.

Photophysical Properties. As seen in Figure 5a, the emission intensity of the four isomers in the presence of AT-DNA at equilibrium differs significantly, which has also been confirmed by steady-state fluorescence spectroscopy (Figure S7 of the Supporting Information), suggesting varying degrees of threading intercalation between the isomers. To exclude the possibility that the difference in emission intensities is an effect of differences in the accessibility to quenching water in the threaded state, emission lifetime measurements were performed, and the results are presented in Table 3. The emission decays look very similar for the stereoisomers having the same chirality on the ip part, and therefore, the decays for **ΔΛ** and **ΛΛ** were fitted to the same two lifetimes, as were the decays for **ΔΔ** and **ΛΔ**, with the pre-exponential factors being allowed to vary independently. For **ΔΛ** and **ΛΛ**, this procedure did not increase the residual norm compared with when the data for each complex was fitted separately, whereas for **ΔΔ** and **ΛΔ**, the residual norm increased by 1−2%. The emission decays are biexponential with a short lifetime of ∼50 ns common to all four isomers, whereas the stereoisomers having the Δ conformation on the ip part displaying a longer second lifetime than those with Λ on the ip part.

The average lifetimes are relatively similar for all four complexes, and comparison of the relative quantum yields and the average lifetimes reveals that the differences in emission intensities

is not an effect of different lifetimes but indicates that there is a difference in threading intercalation binding constants among the four stereoisomers. Assuming the intrinsic lifetime to be the same for all isomers and that 100% of **ΔΔ** is bound, the relative fraction of complex bound by threading intercalation could be calculated by comparison of the ratio between the average lifetime and the relative quantum yield. The values reported in Table 3 are probably somewhat overestimated due to the fact that also groove-bound complexes are weakly luminescent as noted above, but they clearly show that **ΔΔ** has the largest and **ΛΔ** the smallest threading intercalation binding constant of the four isomers.

DISCUSSION

Previously, we have shown that the **ΔΔ** and **ΛΛ** enantiomers of $[\mu\text{-dppzip(phen)}_4\text{Ru}_2]^{4+}$ binds AT-DNA, but not ct-DNA, by threading intercalation. This conclusion was based on the fact that the complex exhibits slow association and dissociation rates characteristic for threading intercalation, as well as light switch properties, in the presence of AT-DNA. The light switch effect, that is, the complex becoming brightly luminescent when bound to DNA, although its emission is quenched in aqueous solution, is for dppz complexes thought to arise from shielding of the phenazine nitrogens on the dppz ligand from hydrogen-bonding water when the dppz moiety is intercalated between the base pairs. In this work, we have confirmed by LD and CD that the **ΔΔ** and **ΛΛ** stereoisomers of $[\mu\text{-dppzip(phen)}_4\text{Ru}_2]^{4+}$ slowly rearrange from an initial groove-bound state, in which the bridging ligand is inclined relative to the plane of the nucleobases, to a threaded intercalated state in which the bridging ligand is essentially perpendicular to the helix axis. This is evidenced by the change in the LD^r of the bridging ligand $\pi \rightarrow \pi^*$ and MLCT bands at 325 and 485 nm, respectively, which become more negative with time, and is supported by the fact the LD^r of the B_E transition around 400 nm and the B_{A2} transition at 260 nm simultaneously becomes more positive. The B_E and B_{A2} transition dipole moments, which are arising mainly from MLCT and $\pi \rightarrow \pi^*$ transitions in the phenanthroline ligands, are for each Ru center oriented in a plane approximately perpendicular to the long axis of the bridging ligand[26] and will thus be oriented more parallel to the DNA helix axis when the bridging ligand rearranges to the threaded state in which the bridging ligand is perpendicular to the DNA helix axis. Moreover, the similar LD^r values at 325 and 485 nm compared with the LD^r at 260 nm for pure AT-DNA is consistent with the bridging ligand being more or less parallel to the DNA bases in the final binding state, but since the orientation of the pure DNA changed significantly upon incubation at 37 °C, an exact value of the angle between the bridging ligand and the DNA helix axis could not be obtained.

For **ΔΔ** and **ΛΔ**, the LD and CD spectral changes are much smaller, and it is difficult to confirm that a rearrangement from the groove-bound state to a threaded intercalated state actually takes place. This is due to the fact that only a small fraction of **ΔΔ** and **ΛΔ** binds by threading intercalation, as judged from kinetic and photophysical data, and hence, the LD and CD spectra are dominated by the groove-bound species also at equilibrium. However, from dissociation kinetic experiments, it is evident that that small fractions of **ΔΔ** and **ΛΔ** indeed bind by threading intercalation.

The results presented here concludes that **ΔΛ** is the best threading intercalator of the investigated isomers, followed by **ΛΛ**, **ΔΔ** and finally **ΛΔ**, with **ΔΔ** and **ΛΔ** being significantly worse threading intercalators than the isomers with Λ configuration on the ip part. Consequently, the optimal configuration is Δ on the intercalating dppz part and Λ on the nonintercalating ip part. The fact that **ΔΛ** is a better threading intercalator than **ΔΔ**, both of which having one ruthenium center with "correct" chirality, shows somewhat surprisingly that the interactions between the phenanthrolines of the nonintercalating half of the complex and the DNA are more important than the interactions with the phenanthrolines of the intercalating dppz part.

The differences in threading intercalation ability could be due to either a better binding of the Δ ip part in the groove or more favorable interactions between the Λ ip part and the DNA in the threaded state. Previously, it has been proposed that the DNA has to change conformation from B-form- to a more A-form-like structure for threading to occur,[16] and it is possible that the groove-bound complex is involved in the initiation of such a conformational change. However, LD and CD data show that the initial binding geometry is strikingly similar for all four isomers, and there is no obvious reason why two of the isomers should bind better in the groove or why the other two should initiate the threading process more efficiently. Moreover, the initial binding geometries in the presence of AT-DNA, where threading occurs, are very similar to the binding geometries in the presence of ct-DNA, where threading does not occur, which further implies that the differences lie in the threaded state instead of the initial state. Therefore, we believe that the differences in threading intercalation ability are due to how well the different isomers fit the binding site in the threaded state, and this is supported by the fact that the dissociation rates are quite different between the different isomers.

It is quite surprising that the LD^r around 260 nm is so similar for all four isomers in the initial state because the LD^r in this region is dominated mainly by the phenanthroline ligands. In this region, the LD^r usually shows large differences between the Δ and Λ enantiomers of the same complex, and only when the plane of the bridging ligand is either parallel or perpendicular to the DNA helix axis will the angle between the DNA helix axis and the B_{A2} transition at 260 nm be the same for the two enantiomers. It is, of course, possible that a deviation from a parallel or perpendicular orientation of one-half of the complex is compensated for by a similar deviation in the opposite direction of the other half of the complex, but it seems very unlikely that this would occur in such a way that the LD^r in the 260 nm region becomes identical for all four isomers. The fact that the LD^r of the bridging ligand becomes more negative when **ΔΛ** and **ΛΛ** rearranges to the threaded state suggests that the plane of the bridging ligand is not perpendicular to the helix axis in the initial state because when the plane of the bridging ligand is perpendicular to the DNA helix axis, so is also the transition dipole moment of the bridging ligand, and the LD^r of this transition cannot possibly become more negative. Therefore, we propose that all isomers of $[\mu\text{-dppzip(phen)}_4\text{Ru}_2]^{4+}$ initially bind in the one of the grooves of the DNA with the normal of the plane of the bridging ligand more or less perpendicular to the DNA helix axis and the long axis of the complex inclined relative the plane of the DNA bases (see Figure S8 of the Supporting Information for a cartoon of the proposed binding mode).

The fact that the chirality on the nonintercalating ip part of the complex seems to control the threading intercalation ability of $[\mu\text{-dppzip(phen)}_4\text{Ru}_2]^{4+}$ explains the reversed enantioselectivity of the homochiral enantiomers of $[\mu\text{-dppzip(phen)}_4\text{Ru}_2]^{4+}$

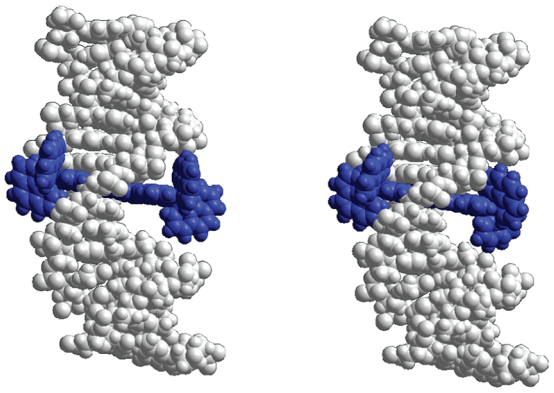

Figure 7. Cartoon illustrating the sterically less congested threading intercalation of **ΔΛ**-$[\mu$-bidppz$(phen)_4Ru_2]^{4+}$ (left) as compared with **ΔΛ**-$[\mu$-dppzip$(phen)_4Ru_2]^{4+}$ (right). The DNA oligomer conformation and the position of the **Δ**-[Ru$(phen)_2$dppz] moiety in the intercalation pocket are identical in the two figures. Bridging ligands bidppz and dppzip are modeled as planar, the former as the syn rotamer. The complexes were manually docked into an intercalation pocket of an 18-mer duplex, created with the Amber force field in the HyperChem 7.52 software package.

compared with those of the parent complex $[\mu$-bidppz$(phen)_4Ru_2]^{4+}$. Previously, it has been proposed that the preference for the ΔΔ enantiomer for threading intercalation of $[\mu$-bidppz$(phen)_4Ru_2]^{4+}$ is an effect of more favorable interactions with the nonintercalating half in the major groove, rather than having the Δ conformation on the intercalating part.[18] However, comparison of the four isomers of $[\mu$-dppzip$(phen)_4Ru_2]^{4+}$, for which we can distinguish the intercalating part from the nonintercalating part due to the asymmetric bridging ligand, clearly indicates that the Δ rather than Λ conformation on the intercalating part is preferable. Because the intercalating parts are identical for the two complexes, it seems likely that this is the case also for $[\mu$-bidppz$(phen)_4Ru_2]^{4+}$, which suggests that the preference for the ΔΔ enantiomer is due to interactions between the DNA and the intercalating half rather than the nonintercalating half, as previously proposed. However, for $[\mu$-dppzip$(phen)_4Ru_2]^{4+}$, the ip part, in which Λ is the most favorable configuration, is controlling the enantioselectivity. This is probably due to the fact that the distance between the ruthenium atoms is shorter for $[\mu$-dppzip$(phen)_4Ru_2]^{4+}$ than for $[\mu$-bidppz$(phen)_4Ru_2]^{4+}$, and when the phenanthrolines of the nonintercalating half of the complex comes closer to the DNA, their interactions with the helix becomes more important, as we previously proposed (see Figure 7 for a cartoon illustrating how the different lengths of the two complexes may affect the interactions with the DNA in the threaded state).[20]

The observation of the light switch effect suggests that the dppz part is protected from solvent in the excited state of the threaded intercalated species, and consequently, the dppz part, and not the ip part, presumably intercalates the DNA. However, the emission lifetime of the threaded state is controlled by the chirality on the ip part. This can be due to either alterations of the binding geometry of the dppz part in the intercalation pocket caused by sterical interactions between the ip part and the DNA or that the interactions between the complex and the DNA alter the excited state in such a way that it becomes more localized to the ip half and is thus affected by the interactions between the ip part of the complex and the DNA. Either way, this shows that the ip part is in close contact with the DNA in the threaded state.

CONCLUSION

In this work, we have investigated the DNA threading intercalation ability of the four stereoisomers of $[\mu$-dppzip$(phen)_4Ru_2]^{4+}$. The isomer with the Δ configuration on the intercalating dppz part and Λ configuration on the nonintercalating ip part is the most efficient threading intercalator of the investigated isomers, which our results indicate is due to a better fit of this isomer in the threading intercalation binding site, rather than a worse fit in the initial groove-bound state. Thus, as the bridging ligand of threading intercalating binuclear ruthenium complexes becomes shorter, as is the case when going from the parent complex $[\mu$-bidppz$(phen)_4Ru_2]^{4+}$ to $[\mu$-dppzip$(phen)_4Ru_2]^{4+}$, the interactions between the phenanthrolines of the nonintercalating part and the DNA become increasingly important and dominate the enantioselectivity. For complexes with longer bridging ligands, on the other hand, the chirality around the intercalating part seems more important, and this is probably the reason for the reversed enantioselectivity for homochiral $[\mu$-dppzip$(phen)_4Ru_2]^{4+}$ compared with $[\mu$-bidppz$(phen)_4Ru_2]^{4+}$.

ASSOCIATED CONTENT

Supporting Information. Absorption spectra of the complexes free in buffer solution, comparison of LD^r and CD spectra immediately after mixing with AT-DNA and ct-DNA, comparison of LD^r of **ΔΔ** and **ΛΔ** in the presence of AT-DNA immediately after mixing and at equilibrium, LD spectra for all isomers in the presence of AT-DNA immediately after mixing and at equilibrium, kinetic traces for association and dissociation in the presence of AT-DNA at 37 and 25 °C, steady state emission spectra in the presence of AT-DNA, cartoon of groove-bound **ΔΔ**. This material is available free of charge via the Internet at http://pubs.acs.org.

AUTHOR INFORMATION

Corresponding Author

*Phone: +46 31 772 30 55. Fax: +46 31 772 38 58. E-mail: lincoln@chalmers.se.

ACKNOWLEDGMENT

This work was funded by the Swedish Research Council (VR).

REFERENCES

(1) Fox, K. R.; Brassett, C.; Waring, M. J. *Biochim. Biophys. Acta* **1985**, *840*, 383–392.
(2) Fox, K. R.; Waring, M. J. *Biochim. Biophys. Acta* **1984**, *802*, 162–168.
(3) Kersten, W.; Kersten, H.; Szybalski., W. *Biochemistry* **1966**, *5*, 236–244.
(4) Smith, C. K.; Davies, G. J.; Dodson, E. J.; Moore, M. H. *Biochemistry* **1995**, *34*, 415–425.
(5) Muller, W.; Crothers, D. M. *J. Mol. Biol.* **1968**, *35*, 251–290.
(6) Nordell, P.; Westerlund, F.; Wilhelmsson, L. M.; Norden, B.; Lincoln, P. *Angew. Chem., Int. Ed* **2007**, *46*, 2203–2206.
(7) Tanious, F. A.; Yen, S. F.; Wilson, W. D. *Biochemistry* **1991**, *30*, 1813–1819.
(8) Krishnamurthy, M.; Gooch, B. D.; Beal, P. A. *Org. Biomol. Chem.* **2006**, *4*, 639–645.
(9) Gooch, B. D.; Krishnamurthy, M.; Shadid, M.; Beal, P. A. *ChemBioChem* **2005**, *6*, 2247–2254.
(10) Gooch, B. D.; Beal, P. A. *J. Am. Chem. Soc.* **2004**, *126*, 10603–10610.

(11) Bourdouxhe-Housiaux, C.; Colson, P.; Houssier, C.; Bailly, C. *Anti-Cancer Drug Des.* **1996**, *11*, 509–525.
(12) Grimm, G. N.; Boutorine, A. S.; Lincoln, P.; Norden, B.; Helene, C. *ChemBioChem* **2002**, *3*, 324–331.
(13) Ossipov, D.; Pradeepkumar, P. I.; Holmer, M.; Chattopadhyaya, J. *J. Am. Chem. Soc.* **2001**, *123*, 3551–3562.
(14) Cline, L. L.; Waters, M. L. *Org. Biomol. Chem.* **2009**, *7*, 4622–4630.
(15) Wilhelmsson, L. M.; Westerlund, F.; Lincoln, P.; Norden, B. *J. Am. Chem. Soc.* **2002**, *124*, 12092–12093.
(16) Nordell, P.; Westerlund, F.; Reymer, A.; El-Sagheer, A. H.; Brown, T.; Norden, B.; Lincoln, P. *J. Am. Chem. Soc.* **2008**, *130*, 14651–14658.
(17) Nordell, P.; Jansson, E. T.; Lincoln, P. *Biochemistry* **2009**, *48*, 1442–1444.
(18) Wilhelmsson, L. M.; Esbjorner, E. K.; Westerlund, F.; Norden, B.; Lincoln, P. *J. Phys. Chem. B* **2003**, *107*, 11784–11793.
(19) Paramanathan, T.; Westerlund, F.; McCauley, M. J.; Rouzina, I.; Lincoln, P.; Williams, M. C. *J. Am. Chem. Soc.* **2008**, *130*, 3752–3753.
(20) Andersson, J.; Li, M. N.; Lincoln, P. *Chem.—Eur. J.* **2010**, *16*, 11037–11046.
(21) Norden, B.; Kubista, M.; Kurucsev, T. *Q. Rev. Biophys.* **1992**, *25*, 51–170.
(22) Westerlund, F.; Nordell, P.; Blechinger, J.; Santos, T. M.; Norden, B.; Lincoln, P. *J. Phys. Chem. B* **2008**, *112*, 6688–6694.
(23) Lutterman, D. A.; Chouai, A.; Liu, Y.; Sun, Y.; Stewart, C. D.; Dunbar, K. R.; Turro, C. *J. Am. Chem. Soc.* **2008**, *130*, 1163–1170.
(24) Westerlund, F.; Nordell, P.; Norden, B.; Lincoln, P. *J. Phys. Chem. B* **2007**, *111*, 9132–9137.
(25) Westerlund, F.; Wilhelmsson, L. M.; Norden, B.; Lincoln, P. *J. Am. Chem. Soc.* **2003**, *125*, 3773–3779.
(26) Lincoln, P.; Broo, A.; Norden, B. *J. Am. Chem. Soc.* **1996**, *118*, 2644–2653.